nature neuroscience

Dendritic patterning by Dscam and synaptic partner matching in the *Drosophila* antennal lobe

Haitao Zhu[1], Thomas Hummel[2,3], James C Clemens[2,3], Daniela Berdnik[1], S Lawrence Zipursky[2] & Liqun Luo[1]

In the olfactory system of *Drosophila melanogaster*, axons of olfactory receptor neurons (ORNs) and dendrites of second-order projection neurons typically target 1 of ~50 glomeruli. Dscam, an immunoglobulin superfamily protein, acts in ORNs to regulate axon targeting. Here we show that Dscam acts in projection neurons and local interneurons to control the elaboration of dendritic fields. The removal of Dscam selectively from projection neurons or local interneurons led to clumped dendrites and marked reduction in their dendritic field size. Overexpression of Dscam in projection neurons caused dendrites to be more diffuse during development and shifted their relative position in adulthood. Notably, the positional shift of projection neuron dendrites caused a corresponding shift of its partner ORN axons, thus maintaining the connection specificity. This observation provides evidence for a pre- and postsynaptic matching mechanism independent of precise glomerular positioning.

Sensory systems use spatial maps in the brain to represent and process information received from the outside world. The organizational principles of olfactory maps in insects and mammals are similar[1]. In *Drosophila*, each ORN typically expresses a single olfactory receptor gene[2–7]. The cell bodies of ORNs expressing the same olfactory receptor gene are dispersed in the olfactory epithelium, whereas their axons converge to a single glomerulus in the antennal lobe (equivalent to the olfactory bulb in vertebrates). ORNs expressing a given olfactory receptor project their axons to a specific glomerulus at a stereotypical position in the antennal lobe[6–9]. Within each glomerulus, ORNs make synapses with dendrites of projection neurons. Typically each projection neuron extends dendrites into a single glomerulus and each glomerulus comprises dendrites from ~3 different projection neurons. Olfactory information is relayed by the projection neurons to higher olfactory centers. The targeting of projection neuron dendrites in the antennal lobe and the stereotypical axonal projection patterns of these neurons in higher brain centers[10,11] are genetically specified by lineage and birth order[12–14]. Hence, the formation of the olfactory map in the antennal lobe involves both specific targeting of ORN axons and projection neuron dendrites (**Fig. 1a**).

How do the spatial maps for ORN axons and projection neuron dendrites form during development? In *Drosophila*, both ORN axons and projection neuron dendrites have substantial self-organizing properties[15–17]. ORN axons and projection neuron dendrites may each form a rigid spatial map based on interactions with cues other than their synaptic partners. The convergence of the two maps in the same spatial position dictates the connection specificities between ORN axons and projection neuron dendrites. Alternatively, ORN axons and projection neuron dendrites may initially form coarse and flexible maps. The two maps register with each other through interactions between ORN axons and projection neuron dendrites, finalizing specific connections.

The molecular basis of olfactory map formation is poorly understood. Indeed, despite the organizational similarity between mammalian and fly maps, odorant receptors in *Drosophila* do not seem to control targeting[18,19] as they do in mammals[20–22]. Hence, the molecular interactions underlying precise targeting must be substantially different in some way. *Dscam*, a gene that generates tens of thousands of isoforms of an immunoglobulin superfamily cell-surface protein[23], is required in ORNs for the targeting of axons to the correct glomeruli[24]. Dscam also has widespread roles in axon guidance and branching[23–27]. However, its role in dendrite development has not been investigated.

Here we show that Dscam regulates the dendritic patterning of projection neurons, as well as that of local interneurons and a specialized set of projection neurons that form large dendritic fields innervating most or all glomeruli. The gain- and loss-of-function experiments were consistent with matched Dscam isoforms promoting repulsive interactions between dendrites of the same cell. The defects in glomerular position induced by Dscam overexpression provided a unique opportunity to investigate whether ORN axon targeting is controlled by glomerular position or by identity. Notably, the change in the projection neuron dendritic map resulted in a corresponding change in the ORN axonal map, such that the connection specificity between projection neurons and ORNs was maintained. This observation provides evidence for a pre- and postsynaptic recognition mechanism independent of precise glomerular positioning.

[1]Howard Hughes Medical Institute and Department of Biological Sciences, Stanford University, Stanford, California 94305, USA. [2]Howard Hughes Medical Institute and Department of Biological Chemistry, the David Geffen School of Medicine at the University of California Los Angeles, Los Angeles, California 90095, USA. [3]Present addresses: Institut fuer Neurobiologie, Universitaet Muenster, Badestr. 9, 48149 Muenster, Germany (T.H.) and Department of Biochemistry, Purdue University, West Lafayette, Indiana 47907, USA (J.C.C.). Correspondence should be addressed to L.L. (lluo@stanford.edu) or S.L.Z. (lzipursky@mednet.ucla.edu).

Received 3 January; accepted 25 January; published online 12 February 2006; doi:10.1038/nn1652

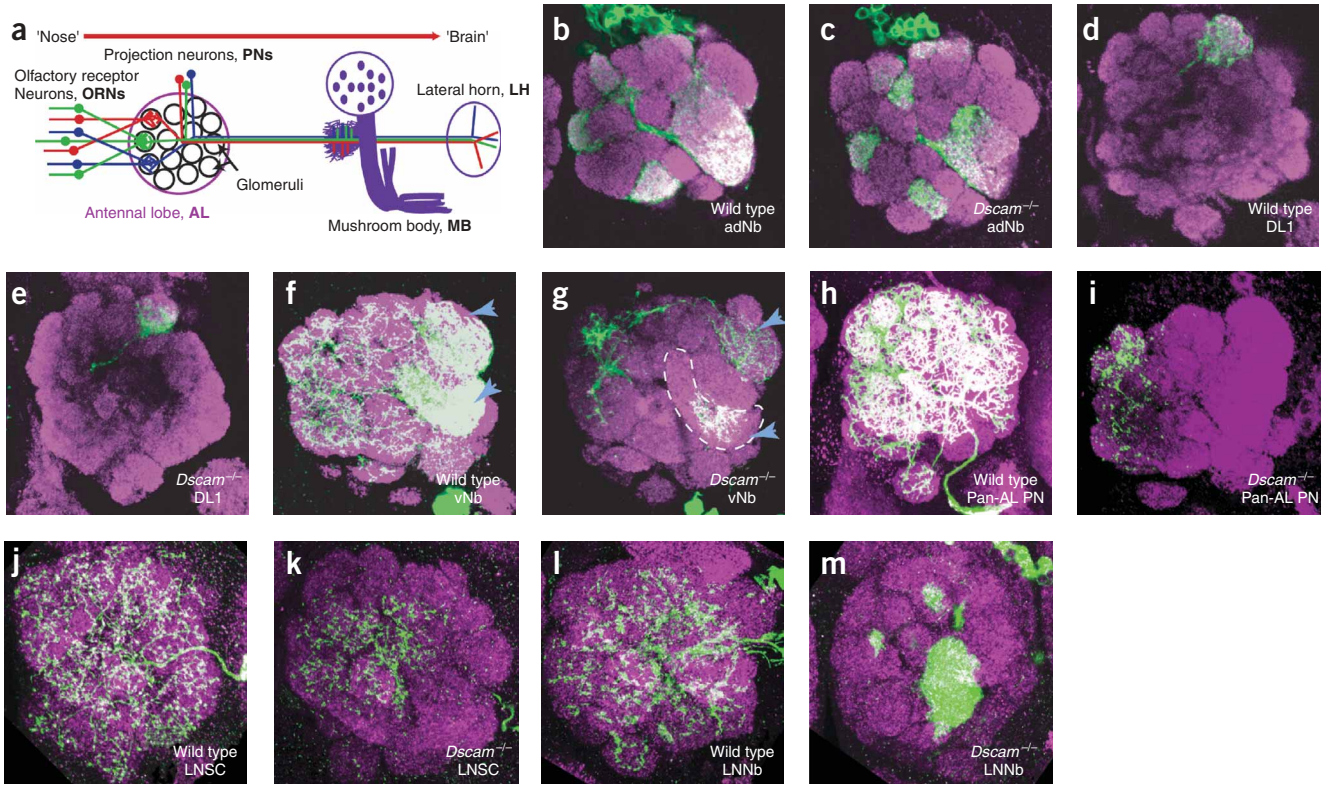

Figure 1 Dscam loss-of-function phenotypes in projection neuron and local interneuron dendrites. (**a**) Schematic of *Drosophila* olfactory system organization. (**b**–**g**) Projection neuron MARCM clones in the wild type (**b**,**d**,**f**) and in *Dscam*$^{-/-}$ mutants (**c**,**e**,**g**), highlighting their dendritic projections in the antennal lobe. (**b**,**c**) Anterodorsal neuroblast (adNb) clones; (**d**,**e**) single-cell DL1 clones; (**f**,**g**) ventral neuroblast (vNb) clones. Arrowheads indicate DA1 (top) and VA1lm glomeruli. The boundary of the VA1lm glomerulus is indicated by dashed line in **g**. (**h**,**i**) Pan-AL single-cell clones. (**j**,**k**) Local interneuron single-cell clones (LNSC). (**l**,**m**) Local interneuron neuroblast clones (LNNb). All images are representative of at least 15 samples with similar phenotypes, except **i** which is representative of 3 samples. All images in this and subsequent figures are confocal sections of the antennal lobe oriented such that dorsal is up and medial is to the left. Unless otherwise noted, brains in this and subsequent figures are stained with rat antibody to mCD8 to label projection neurons of MARCM clones (green) and counterstained with mouse antibody nc82 to label the neuropil (magenta). PN, projection neuron.

RESULTS

Dendritic elaboration of projection neurons requires Dscam

We found that Dscam is highly expressed in the developing projection neuron dendrites in the antennal lobe before ORN axon invasion (**Supplementary Fig. 1** online). To study the Dscam loss-of-function phenotype in projection neuron dendrites, we used the mosaic analysis with a repressible cell marker (MARCM) method[28] to generate green fluorescent protein (GFP)-labeled *Dscam* homozygous mutant projection neuron clones using Gal4-GH146, which labels 90 of ~150 projection neurons (refs. 12,29). For the projection neuron analysis, we used two distinct *Dscam* alleles generated in different genetic backgrounds, *Dscam*^{P1} and *Dscam*^{23}. Both alleles are protein-null[23,24].

Neuroblast clone analysis did not reveal obvious mistargeting errors in *Dscam* mutant projection neurons (compare **Fig. 1b** with **Fig. 1c**; data not shown). To study the projection neuron dendritic innervation at single-cell resolution, we generated wild-type and *Dscam* mutant single-cell clones for projection neurons innervating the DL1 glomerulus. Compared with their wild-type counterparts (**Fig. 1d**), the dendrites of *Dscam* mutant cells innervated the correct DL1 glomerulus but the dendritic elaboration was reduced, often only partially innervating the DL1 glomerulus (**Fig. 1e**; 17 of 20). Analysis of projection neurons from the ventral neuroblast (vNb) clones confirmed and extended the requirement for Dscam in dendritic elaboration. The vNb gives rise to six GH146-positive cells, at least one each innervating the glomeruli DA1 and VA1lm[10,12]. In *Dscam* mutant vNb clones, the innervation of DA1 and VA1lm was strongly reduced and was often only partial within the glomeruli (compare **Fig. 1f** with **Fig. 1g**, arrowheads; 13 of 15). These findings indicated that Dscam promoted projection neuron dendrite elaboration within the correct target glomerulus but was not required for the selection of the appropriate glomerulus to innervate.

Formation of large dendritic fields requires Dscam

Two classes of neurons, local interneurons and a pan–antennal-lobe (pan-AL) projection neuron, elaborate expansive dendritic fields (**Fig. 1h–m**). Indeed, the dendrites of single cells ramified throughout the AL and innervated most or all glomeruli (**Fig. 1h,j**). The pan-AL projection neuron is derived from the vNb[10]; we visualized it with GH146 either in vNb clones (**Fig. 1f**) or in single-cell clones (**Fig. 1h**). In *Dscam* mutant vNb (**Fig. 1g**, 15 of 15) or single-cell clones (**Fig. 1i**, 3 of 3), the extent of the dendritic field was substantially reduced: dendrites only innervated the medial part of the antennal lobe. As in uniglomerular projection neurons, the dendrites were frequently clumped.

To test whether the large dendritic fields formed by local interneurons require Dscam, we performed MARCM analysis using the local interneuron marker *Gal4-GH298*[29]. All the wild-type single-cell clones we analyzed elaborated a uniform distribution of dendrites across the entire antennal lobe ($n = 12$; **Fig. 1j**). By contrast, single Dscam mutant cells (32/32; homozygous for one of the three null alleles, *Dscam*^{21},

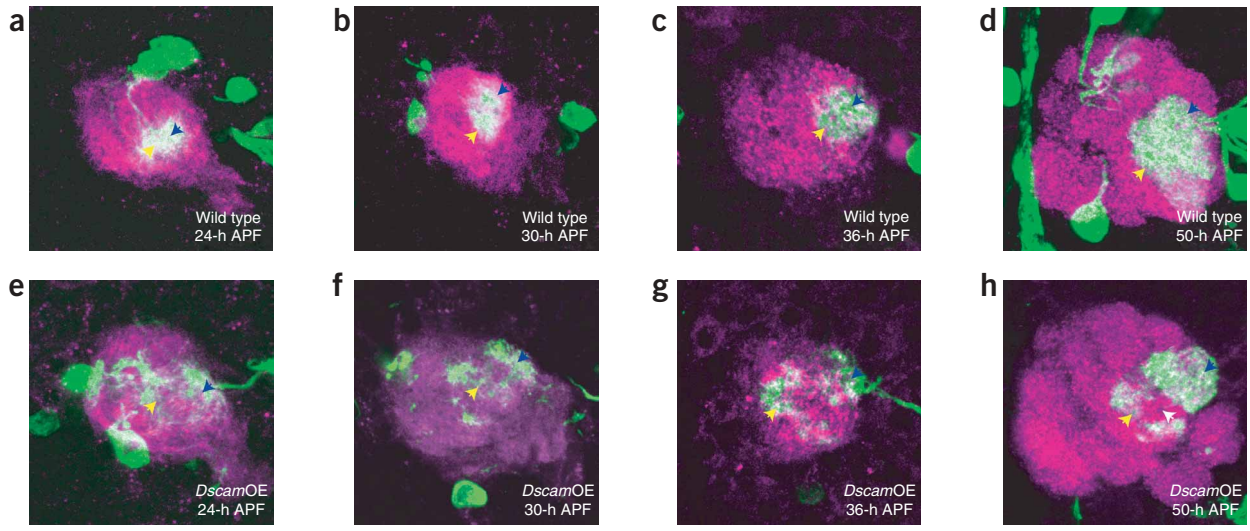

Figure 2 Projection neurons overexpressing Dscam elaborate more diffuse dendrites in the developing antennal lobe. (**a**–**h**) Representative confocal images of dendrites of Mz19$^+$ projection neurons expressing only mCD8-GFP (**a**–**d**) or together with the *Dscam1-30-30-1* transgene (**e**–**h**) at different developmental stages. Consistent results were obtained for different samples examined ($n \geq 8$). Yellow and blue arrows, dendritic mass of VA1d and DA1, respectively. White arrow in **h**, ectopic glomerulus between VA1d and DA1. Pupal brains from 24-h (**a**,**e**) and 30-h (**b**,**f**) APF were stained with rabbit antibody to GFP (green) to label MARCM clones and with rat antibody to N-cadherin (magenta) to label the developing antennal lobe.

Dscam[23] or *Dscam*[33]) did not evenly innervate all glomeruli. Indeed, as in pan-AL projection neurons, dendrites in lateral regions were more affected than those in the medial region (**Fig. 1k**). *Dscam* mutant neuroblast clones containing 5–10 local interneurons also showed severe clumping defects of dendritic patterning (**Fig. 1m**, compared with control in **Fig. 1l**, 32 of 32): a massive aggregate of dendrites formed as a condensed sphere-like structure within the antennal lobe.

In summary, these loss-of-function analyses indicated that Dscam was required for the elaboration of large dendritic fields within the antennal lobe. The reduction in the extent of the dendritic fields seen in mutant local interneurons and pan-AL projection neurons was similar to that observed for uniglomerular projection neurons. By contrast, although mutant uniglomerular projection neurons showed defects of dendritic elaboration within the appropriate glomerulus, *Dscam* mutant local interneuron dendrites and pan-AL projection neurons frequently did not innervate many glomeruli.

Dscam overexpression causes dendrite diffusion in pupa

To assess the effects of overexpressing *Dscam* transgenes in projection neuron dendrites, we used Mz19-Gal4 (ref. 15) to target *Dscam* expression in projection neurons innervating three neighboring glomeruli (**Fig. 2**): VA1d and DA1 on the anterior surface and DC3 posterior to VA1d. We visualized the dendrites at different developmental stages. As early as 24 h after puparium formation (24-h APF), when dendritic arborization of the Mz19-positive (Mz19$^+$) projection neurons could first be visualized, the wild-type dendrites formed two overlapping dendritic arbors adjacent to each other at the anterior surface of the antennal lobe. These arbors represented glomeruli VA1d and DA1 (**Fig. 2a**; ref. 15). By contrast, in projection neurons overexpressing a single Dscam isoform (encoded by the transgene *Dscam1-30-30-1*, which is named according to its distinct combinations of the variable exons; ref. 30), the two dendritic arbors were clearly separable by 24-h APF (**Fig. 2e**). Furthermore, at this early stage, dendrites extended over broader regions of the antennal lobe than those in the wild type in all samples examined ($n = 14$).

During later developmental stages, the dendrites of wild-type Mz19$^+$ projection neurons gradually refined and form two distinct glomeruli by 50-h APF; in contrast, the separation of dendrites persisted in projection neurons overexpressing *Dscam* (**Fig. 2f–h** compared with **Fig. 2b–d**). These phenotypes were seen before the onset of the majority of olfactory receptor gene expression and before the maturation of synaptic connections in the antennal lobe[15]; thus, it is unlikely that the overexpression phenotype involves sensory input or synaptic activity.

Dscam overexpression shifts dendritic position in adult

Using Gal4-Mz19, we examined adult antennal lobes in which Dscam isoforms were expressed and found a striking defect in glomerular organization. Although DA1 and DC3 dendrites were at their normal positions in the antennal lobe, VA1d dendrites were often shifted to a more ventral position on the anterior surface and were now separated from DA1 dendrites by another glomerulus (**Fig. 3**; compare **Fig. 3a** and **b**, arrowhead). Therefore, the overexpression of *Dscam* seemed to cause a change in the spatial position of VA1d projection neuron dendrites in the adult antennal lobe.

To examine whether this overexpression phenotype is unique to a specific isoform, we tested transgenes expressing different Dscam isoforms. To control for the variability of transgene expression level, we tested two independent inserts for each transgene isoform. We found that the overexpression phenotypes were present in all isoforms tested, with variable penetrance from 5% to 85% (**Fig. 3b–e**, quantified in **Fig. 3g**). These results indicated that the ventral shift of VA1d projection neuron dendrites was not unique to a specific Dscam isoform.

Overexpressed Dscam acts autonomously in dendritic shift

How does Dscam overexpression alter the glomerular pattern? It is possible that the positional shift of VA1d dendrites is caused by the isoform-specific repulsive interaction between the neighboring DA1 and VA1d dendrites. If this were true, one would predict that overexpressing only a single isoform of Dscam in both DA1 and VA1d at the

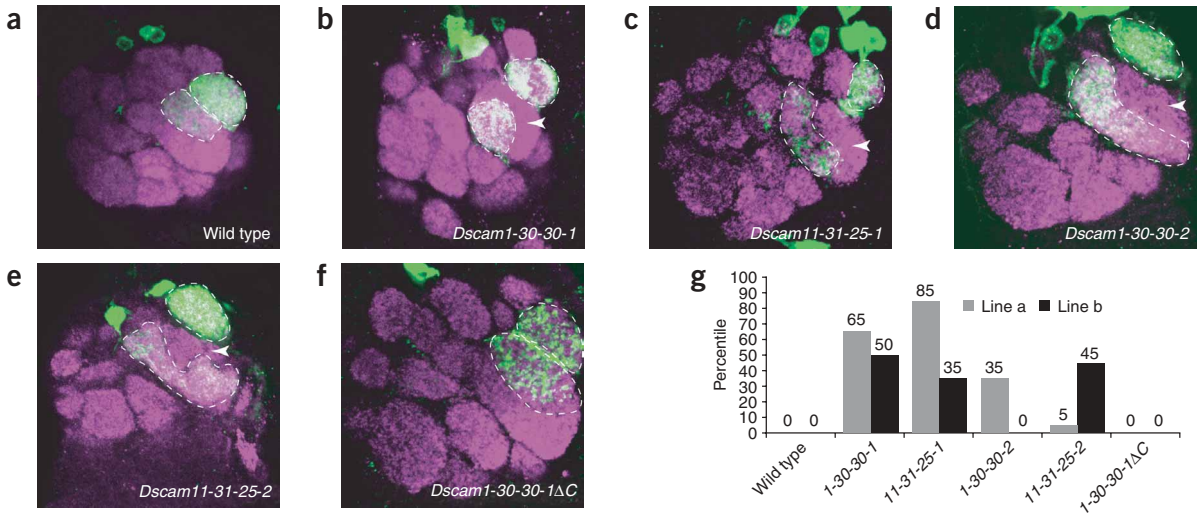

Figure 3 Dscam overexpression in Mz19$^+$ projection neurons results in specific dendritic position shift in the adult antennal lobe. (**a**–**f**) Representative confocal images of Mz19$^+$ projection neurons expressing mCD8-GFP alone (**a**) or with different *Dscam* transgenes (**b**–**f**), highlighting their dendritic projections in the antennal lobe. Transgenes tested include *Dscam1-30-30-1* (**b**), *Dscam11-31-25-1* (**c**), *Dscam1-30-30-2* (**d**), *Dscam11-31-25-2* (**e**) and *Dscam1-30-30-1C* with the cytoplasmic domain replaced by GFP (**f**). *Dscam1-30-30-1* and *Dscam1-30-30-2* have identical extracellular domains and different transmembrane domains. The same is true for the other two Dscam isoforms. Arrowheads, ectopic glomeruli between DA1 and VA1d. In **f**, brains were stained with rabbit antibody to GFP (green) and with mouse antibody nc82 (magenta). (**g**) Quantification of the penetrance of *Dscam* transgene overexpression phenotype represented in percentile ($n = 20$ for each transgenic insertion tested). Two independent insertions (**a**,**b**; gray and black, respectively) were quantified for each transgene.

same time could cause the phenotype. Another possibility is that DA1 dendrites overexpressing *Dscam* repel the VA1d dendrites or attract more ventral VA1lm dendrites. Alternatively, *Dscam* overexpression may affect VA1d dendritic targeting autonomously.

To distinguish between these three possibilities, we used MARCM to express *Dscam1-30-30-1* in subsets of Mz19$^+$ projection neurons. These cells originate from two distinct cell lineages: the projection neurons innervating the DA1 glomerulus are from the lateral neuroblast whereas those innervating VA1d and DC3 are from the anterodorsal neuroblast. This allowed us to express *Dscam* transgenes in either the projection neurons innervating DA1 or in those innervating VA1d and DC3, in MARCM neuroblast clones (**Fig. 4**). The overexpression of *Dscam1-30-30-1* in only the projection neurons innervating DA1 did not result in a ventral shift of the VA1d glomerulus, as indicated by an ORN axon marker for VA1d (**Fig. 4a**, $n = 10$; see **Fig. 5** for detail of the ORN axon marker). This observation excluded the possibility that the overexpression of *Dscam* in projection neurons innervating DA1 repels VA1d dendrites or attracts VA1lm dendrites in a non–cell-autonomous manner. When we overexpressed *Dscam* transgenes in VA1d and DC3, we observed the ventral shift of the VA1d dendrites and the ORN axon marker in 42% of the brain hemispheres examined (**Fig. 4b**, $n = 12$). In contrast, the posterior DC3 glomerulus remained unchanged and in contact with the ventrally shifted VA1d glomerulus (data not shown). This result argued against the possibility that the phenotype was caused simply by a single isoform of Dscam mediating repulsive interactions between DA1 and VA1d dendrites.

To investigate whether Dscam-mediated signaling is required for the shift in glomerular position, we generated a variant of the *Dscam1-30-30-1* transgene in which we replaced the cytoplasmic domain of Dscam with GFP. We tested five different insertion lines of the transgene and did not observe any shift in glomerular position, even though the fusion proteins were highly expressed in the dendrites (**Fig. 3f**,**g**). This result, in combination with the above MARCM overexpression results, indicated that overexpressed Dscam acts as a cell-surface receptor in the dendrites of VA1d projection neurons to affect the neuron's dendritic position in the antennal lobe. The fact that loss-of-function Dscam does not result in a positional shift suggested one of two possibilities: either Dscam acts in a redundant manner in this process or Dscam overexpression activates or inhibits, in a non–physiologically relevant fashion, a signaling pathway that normally regulates glomerular position.

Partner ORN axons follow shifted dendrites

The shift of position of the VA1d projection neuron dendrites caused by the overexpression of Dscam in these neurons offered a unique opportunity to investigate the logic of olfactory circuit assembly. Because projection neuron dendrites form a coarse spatial map before ORN axons invade[15], ORN axons could use the projection neuron dendritic map as a cue to determine their spatial position in the antennal lobe. To date, however, there is no experimental support for this hypothesis. Alternative proposals are that ORN axons recognize non–projection neuron cues within or surrounding the antennal lobe and/or that they self-organize through axon-axon interaction[17,31] to reach their spatially invariant targets.

The overexpression of *Dscam* in projection neuron alters the initial spatial map of the projection neuron dendrites before ORN invasion; therefore, we can ask whether the change in the spatial map of the projection neuron dendrites affects the targeting of the corresponding ORN axons. If projection neuron dendritic maps were used as cues for ORN axon targeting, one would predict a corresponding shift of ORN axon position. Alternatively, if the spatial positions of ORN axons were solely determined by interactions among ORN axons or with non–projection neuron cues, changing the spatial map of projection neuron dendrites would lead to a mismatch of projection neuron dendrites and ORN axons and would result in a change in connection specificity.

To distinguish between these two possibilities, we examined ORN axon innervation patterns in the antennal lobe in response to the

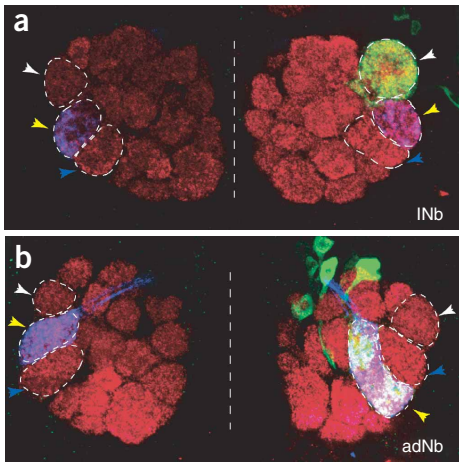

Figure 4 MARCM overexpression of the *Dscam* transgene in projection neuron dendrites and its effect on ORN axons. Axonal projections of Or88a ORNs were labeled with the *Or88a-CD2* transgene and visualized with an antibody to CD2 (blue; becomes white when overlaid with nc82 staining (red) and mCD8-GFP staining (green)). White-dashed straight lines, midlines. White-dashed circles, boundaries of the glomeruli of interest (DA1, VA1d and VA1lm). White, yellow and blue arrows, glomeruli DA1, VA1d and VA1lm, respectively. (**a**) Axonal projections of Or88a ORNs were compared in brain hemispheres with no clones (left, $n > 20$) and with lateral neuroblast MARCM clones (innervating DA1, green) overexpressing the *Dscam-1-30-30-1* transgene (right). Note the normal position of Or88a ORN axons (in 10 of 10 samples examined). (**b**) Axonal projections of Or88a ORNs were compared in brain hemispheres with no clones (left, $n > 20$) and with anterodorsal neuroblast MARCM clones (innervating VA1d; green, looks white and magenta because of overlaying with nc82 in red and Or88a in blue) overexpressing the *Dscam1-30-30-1* transgene (right). Note the ventral shift of VA1d dendrites and the Or88a ORN axons (in 5 of 12 samples examined).

dendritic map shift induced by Dscam overexpression in projection neuron dendrites. The ORNs innervating the VA1d glomerulus express Or88a (ref. 17). To label these ORN axons, we used the transgene *Or88a-CD2* in which the Or88a promotor drives the expression of the membrane marker CD2 (D.B. and L.L., unpublished data). In the same brain, Mz19$^+$ projection neurons were labeled by the membrane marker mCD8-GFP using the Gal4/UAS system. In the wild type, Or88a axons synapsed with Mz19$^+$ projection neuron dendrites innervating VA1d, which is adjacent to the DA1 glomerulus (**Fig. 5a**). In 13 brain hemispheres where Mz19$^+$ projection neurons also overexpressed *Dscam*, the spatial position of the VA1d projection neuron dendrites shifted ventrally, away from the DA1 glomerulus. Notably, Or88a axons shifted to a ventral position accordingly in each case, maintaining the correct connections with the VA1d projection neuron dendrites (**Fig. 5b**). In the seven hemispheres in which Dscam overexpression did not induce a dendritic shift, Or88a axon targeting was normal. These results demonstrated that Or88a axons recognized VA1d projection neuron dendrites, thereby maintaining their connection specificity even when these dendrites were shifted to a different position.

Overexpressing *Dscam* in Mz19$^+$ projection neurons shifted the VA1d dendrites to a ventral position equivalent to VA1lm, which is normally innervated by ORN axons expressing Or47b (**Fig. 5c**). Would Or47b axons still innervate the same position in the antennal lobe and therefore connect incorrectly with the ventrally shifted VA1d projection neuron dendrites? Or would they avoid the ventrally shifted VA1d dendrites and target a new position? To address this question, we labeled the Or47b axons using the transgene *Or47b-CD2* (ref. 16). We found that, in each hemisphere, when Dscam overexpression caused a ventral shift of VA1d dendrites ($n = 12$), Or47b axons shifted to a dorsal position and innervated the glomerulus situated ectopically between DA1 and VA1d, avoiding the VA1d dendrites completely (**Fig. 5d**). In hemispheres where no projection neuron dendritic position shift occurred, Or47b axons targeted normal positions ($n = 8$). Note that for this VA1lm glomerulus, neither the pre- nor the postsynaptic partners had been subjected to any genetic modifications. Their positional shifts were the sole result of the expression of Dscam in projection neurons in glomeruli neighboring VA1lm.

Together, these data supported the notion that glomerular targeting, at least in the two ORN classes examined, requires specific recognition between ORN afferents and projection neuron dendrites.

DISCUSSION

Dscam function in dendritic patterning

Individual neurons express different arrays of isoforms in a largely stochastic fashion[27,32]. It is proposed that such expression provides

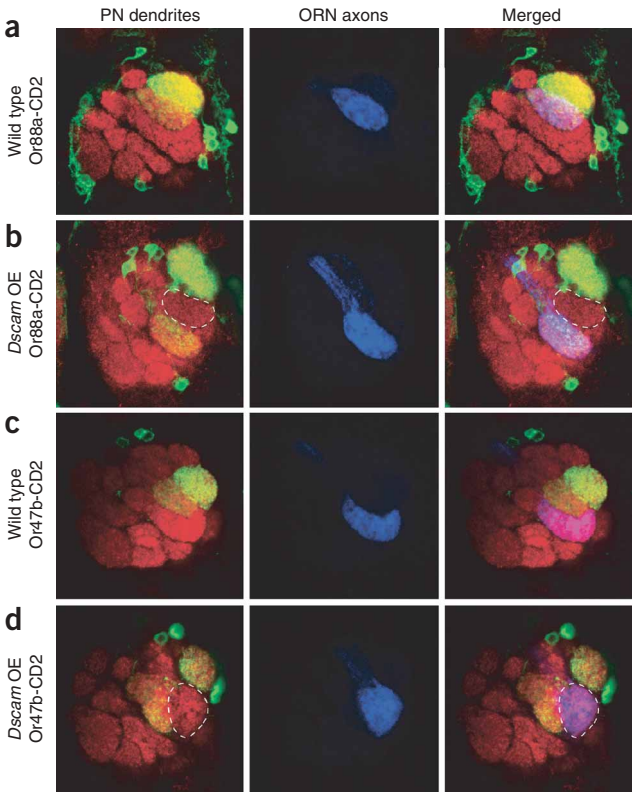

Figure 5 Shift of spatial position of projection neuron dendrites causes a corresponding shift of its partner ORN axons. (**a**–**d**) Axon projections from Or88a (**a**,**b**; targeting the VA1d glomerulus) and Or47b (**c**,**d**; targeting the VA1lm glomerulus) ORNs in brain hemispheres where Gal4-Mz19 drives expression of mCD8-GFP alone (**a**,**c**) or together with *Dscam1-30-30-1 transgene* (**b**,**d**). White-dashed lines, ectopic glomerulus between VA1d and DA1 in *Drosophila* with *Dscam1-30-30-1* transgene expression (**b**,**d**). ORN axonal projections were labeled with the Or88a-CD2 (**a**,**b**; middle and right panels) and Or47b-CD2 (**c**,**d**; middle and right panels) transgenes, respectively, and visualized with an antibody to CD2 (blue).

each neuron with a unique identity[32]. Biochemical studies demonstrate that Dscam promotes isoform-specific binding: isoforms sharing the same extracellular domain bind to each other, whereas isoforms that are different do not[30]. Furthermore, interactions between identical Dscam proteins seem to promote contact-dependent repulsion[25,30]. One phenotype in the Dscam mutant axon is the failure to segregate sister branches[24], which is also the case for projection neuron axons (**Supplementary Fig. 2** online).

How might Dscam contribute to dendrite branching? To efficiently innervate the target areas, some neurons possess an intraneuronal tiling mechanism such that dendritic branches of the same neuron do not overlap[33]. On the basis of expression studies in other neurons[27,32], we propose that the array of Dscam isoforms expressed on a dendrite's surface provides each projection neuron and local interneuron with a mechanism by which to distinguish its own dendrites from those of neighboring cells. Thus, Dscam isoforms expressed on sister branches will be the same; however, they will share little, if any, overlap with the isoforms expressed on dendrites of other projection neurons or local interneurons innervating the same glomerulus. Thus, Dscam diversity provides a mechanism by which dendrites from the same neuron can avoid each other as they elaborate their receptive fields, while overlapping with dendritic processes of other cells within the neuropil.

Implications for the logic of olfactory circuit assembly

Developmental studies have led to a model in which ORNs and projection neurons initially develop spatial maps that are independent of each other[15–17]. When the two spatial maps converge, the connection specificity between a given ORN–projection neuron pair can be determined solely by matching the positional coordinates of the respective spatial maps for ORN axons and projection neuron dendrites. Such an extreme model would predict that if a change is made to the positions of projection neuron dendrites before and independent of the arrival of ORN axons, the positional maps of ORN axons and projection neuron dendrites would be misaligned. Under these circumstances, ORN axons should innervate projection neuron dendrites positioned as they would be in the wild type, rather than as they are in the reordered state; thus the ORN axons would select the incorrect target. Alternatively, these two maps may be rather coarse and specific recognition between appropriate ORN axons and their dendritic targets may be required to refine the map.

Our findings that changing the spatial map of the projection neuron dendrites also leads to corresponding changes of the ORN axon map strongly argues against a strict spatially regulated matching of the afferent axonal and dendritic maps. Our data indicate that ORN axons are influenced by their corresponding postsynaptic projection neuron dendrites in determining their spatial position in the antennal lobe, at least at the local level for the two classes of ORNs analyzed. This finding by no means contradicts the contribution of projection neuron–independent mechanisms in ORN axon targeting. Such mechanisms may be used to set up a coarse map for the ORN axons, limiting the approximate spatial position that a given ORN axon can target. ORN axons would then be faced with only a few projection neuron dendritic targets in the neighborhood, which they can sample through ORN–projection neuron recognition in order to solidify the final synaptic partners. Sensory input and synaptic activity are unlikely to play a role in matching ORN axons and projection neuron dendrites because this process is completed before olfactory receptor expression and synaptic maturation[15]. It is more likely that these processes recognize each other through yet to be identified 'chemoaffinity tags' (ref. 34).

METHODS

Clonal analysis. The MARCM method was applied as described previously[28]. Briefly, *Dscam* alleles were placed transheterozygous to Gal80 on the FRT 42D chromosome. Flipase activity induced by heat shock causes mitotic recombination of the FRT chromosomes such that one of the daughter cells becomes homozygous for *Dscam* and simultaneously loses Gal80. This cell can therefore be labeled by the Gal4/UAS system. For projection neuron analysis, *Drosophila* were heat-shocked between 0 and 18 h after larval hatching for 1.5 h at 37 °C. Adult flies were dissected 5–7 d after eclosion. Genotype: *hsFlp, UAS-mCD8GFP;FRT42D, Dscam, GH146 /FRT42D, Gal80*. Mitotic clones in local interneurons were induced in the first and second instar larvae of the following genotype: *hsFlp; FRT42D, Dscam /FRT42D, Gal80; GH298-Gal4, UAS-mCD8GFP/+*. Heat shocks were carried out at 37 °C for 20 min. Induced clones were analyzed in dissected brains of adult flies 5 d after eclosion.

Transgenes. Dscam cDNAs encoding the full-length isoforms 1-30-30-1 and 1-30-30-2 were isolated as 6.8-kilobase (kb) AseI-SpeI restriction fragments, blunted and then ligated into blunted EcoRI and XbaI sites of the *Drosophila* transgene vector pUAST. Expression constructs encoding 11-31-25 isoforms were subsequently created by replacing the 1.9-kb KpnI-XhoI fragment, containing the 1-30-30 sequences, with a partially digested 1.9-kb KpnI-XhoI fragment encoding the 11-31-25 isoform. *Dscam1-30-30-1C* was created by replacing the C-terminal 358 amino acids of the cytoplasmic domain with GFP coding sequence by polymerase chain reaction. These constructs were introduced into the *Drosophila* genome using standard germline transformation procedures.

Immunochemistry. The procedures for fixation, immunochemistry and imaging were as described previously[12,27].

Note: Supplementary information is available on the Nature Neuroscience website.

ACKNOWLEDGMENTS

We thank E. Buchner for antibodies; and T. Komiyama, C. Potter, B. Tasic, T. Clandinin and K. Shen for comments on the manuscript. H.Z. is a recipient of an individual Kirschstein National Research Service Award (NRSA) postdoctoral fellowship. L.L. and S.L.Z. are investigators of the Howard Hughes Medical Institute. This work was supported by the US National Institutes of Health (grants R01-DC005982 to L.L. and R01-DC006485 to S.L.Z.).

COMPETING INTERESTS STATEMENT

The authors declare that they have no competing financial interests.

Published online at http://www.nature.com/natureneuroscience/
Reprints and permissions information is available online at http://npg.nature.com/reprintsandpermissions/

1. Hildebrand, J.G. & Shepherd, G.M. Mechanisms of olfactory discrimination: converging evidence for common principles across phyla. *Annu. Rev. Neurosci.* **20**, 595–631 (1997).
2. Vosshall, L.B., Amrein, H., Morozov, P.S., Rzhetsky, A. & Axel, R. A spatial map of olfactory receptor expression in the *Drosophila* antenna. *Cell* **96**, 725–736 (1999).
3. Clyne, P.J. *et al.* A novel family of divergent seven-transmembrane proteins: candidate odorant receptors in *Drosophila*. *Neuron* **22**, 327–338 (1999).
4. Gao, Q. & Chess, A. Identification of candidate *Drosophila* olfactory receptors from genomic DNA sequence. *Genomics* **60**, 31–39 (1999).
5. Goldman, A.L., Van der Goes van Naters, W., Lessing, D., Warr, C.G. & Carlson, J.R. Coexpression of two functional odor receptors in one neuron. *Neuron* **45**, 661–666 (2005).
6. Couto, A., Alenius, M. & Dickson, B.J. Molecular, anatomical and functional organization of the *Drosophila* olfactory system. *Curr Biol* (2005).
7. Fishilevich, E. & Vosshall, L.B. Genetic and functional subdivision of the *Drosophila* antennal lobe. *Curr. Biol.* **15**, 1548–1553 (2005).
8. Vosshall, L.B., Wong, A.M. & Axel, R. An olfactory sensory map in the fly brain. *Cell* **102**, 147–159 (2000).
9. Gao, Q., Yuan, B. & Chess, A. Convergent projections of *Drosophila* olfactory neurons to specific glomeruli in the antennal lobe. *Nat. Neurosci.* **3**, 780–785 (2000).
10. Marin, E.C., Jefferis, G.S.X.E., Komiyama, T., Zhu, H. & Luo, L. Representation of the glomerular olfactory map in the *Drosophila* brain. *Cell* **109**, 243–255 (2002).
11. Wong, A.M., Wang, J.W. & Axel, R. Spatial representation of the glomerular map in the *Drosophila* protocerebrum. *Cell* **109**, 229–241 (2002).
12. Jefferis, G.S., Marin, E.C., Stocker, R.F. & Luo, L. Target neuron prespecification in the olfactory map of *Drosophila*. *Nature* **414**, 204–208 (2001).

13. Komiyama, T., Johnson, W.A., Luo, L. & Jefferis, G.S. From lineage to wiring specificity: POU domain transcription factors control precise connections of *Drosophila* olfactory projection neurons. *Cell* **112**, 157–167 (2003).
14. Marin, E.C., Watts, R.J., Tanaka, N.K., Ito, K. & Luo, L. Developmentally programmed remodeling of the *Drosophila* olfactory circuit. *Development* **132**, 725–737 (2005).
15. Jefferis, G.S. *et al*. Developmental origin of wiring specificity in the olfactory system of *Drosophila*. *Development* **131**, 117–130 (2004).
16. Zhu, H. & Luo, L. Diverse functions of N-cadherin in dendritic and axonal terminal arborization of olfactory projection neurons. *Neuron* **42**, 63–75 (2004).
17. Komiyama, T., Carlson, J.R. & Luo, L. Olfactory receptor neuron axon targeting: intrinsic transcriptional control and hierarchical interactions. *Nat. Neurosci.* **7**, 819–825 (2004).
18. Dobritsa, A.A., van der Goes van Naters, W., Warr, C.G., Steinbrecht, R.A. & Carlson, J.R. Integrating the molecular and cellular basis of odor coding in the *Drosophila* antenna. *Neuron* **37**, 827–841 (2003).
19. Wang, J.W., Wong, A.M., Flores, J., Vosshall, L.B. & Axel, R. Two-photon calcium imaging reveals an odor-evoked map of activity in the fly brain. *Cell* **112**, 271–282 (2003).
20. Mombaerts, P. *et al*. Visualizing an olfactory sensory map. *Cell* **87**, 675–686 (1996).
21. Wang, F., Nemes, A., Mendelsohn, M. & Axel, R. Odorant receptors govern the formation of a precise topographic map. *Cell* **93**, 47–60 (1998).
22. Feinstein, P., Bozza, T., Rodriguez, I., Vassalli, A. & Mombaerts, P. Axon guidance of mouse olfactory sensory neurons by odorant receptors and the beta2 adrenergic receptor. *Cell* **117**, 833–846 (2004).
23. Schmucker, D. *et al*. Dscam is an axon guidance receptor exhibiting extraordinary molecular diversity. *Cell* **101**, 671–684 (2000).
24. Hummel, T. *et al*. Axonal targeting of olfactory receptor neurons in *Drosophila* is controlled by Dscam. *Neuron* **37**, 221–231 (2003).
25. Wang, J., Zugates, C.T., Liang, I.H., Lee, C.H. & Lee, T. *Drosophila* Dscam is required for divergent segregation of sister branches and suppresses ectopic bifurcation of axons. *Neuron* **33**, 559–571 (2002).
26. Wang, J. *et al*. Transmembrane/juxtamembrane domain-dependent Dscam distribution and function during mushroom body neuronal morphogenesis. *Neuron* **43**, 663–672 (2004).
27. Zhan, X.L. *et al*. Analysis of Dscam diversity in regulating axon guidance in *Drosophila* mushroom bodies. *Neuron* **43**, 673–686 (2004).
28. Lee, T. & Luo, L. Mosaic analysis with a repressible cell marker for studies of gene function in neuronal morphogenesis. *Neuron* **22**, 451–461 (1999).
29. Stocker, R.F., Heimbeck, G., Gendre, N. & de Belle, J.S. Neuroblast ablation in *Drosophila* P[GAL4] lines reveals origins of olfactory interneurons. *J. Neurobiol.* **32**, 443–456 (1997).
30. Wojtowicz, W.M., Flanagan, J.J., Millard, S.S., Zipursky, S.L. & Clemens, J.C. Alternative splicing of *Drosophila* Dscam generates axon guidance receptors that exhibit isoform-specific homophilic binding. *Cell* **118**, 619–633 (2004).
31. Feinstein, P. & Mombaerts, P. A contextual model for axonal sorting into glomeruli in the mouse olfactory system. *Cell* **117**, 817–831 (2004).
32. Neves, G., Zucker, J., Daly, M. & Chess, A. Stochastic yet biased expression of multiple Dscam splice variants by individual cells. *Nat. Genet.* **36**, 240–246 (2004).
33. Jan, Y.N. & Jan, L.Y. The control of dendrite development. *Neuron* **40**, 229–242 (2003).
34. Sperry, R.W. Chemoaffinity in the orderly growth of nerve fiber patterns and connections. *Proc. Natl. Acad. Sci. USA* **50**, 703–710 (1963).